



HAL
open science

Thermomechanical Properties of Copper-Carbon Nanofibre Composites Prepared by Spark Plasma Sintering and Hot Pressing

Jennifer M. Ullbrand, José M. Córdoba, Javier Tamayo-Ariztondo, María R. Elizalde, Mats Nygren, Jon M. Molina-Aldareguia, Magnus Odén

► **To cite this version:**

Jennifer M. Ullbrand, José M. Córdoba, Javier Tamayo-Ariztondo, María R. Elizalde, Mats Nygren, et al.. Thermomechanical Properties of Copper-Carbon Nanofibre Composites Prepared by Spark Plasma Sintering and Hot Pressing. *Composites Science and Technology*, 2010, 70 (16), pp.2263. 10.1016/j.compscitech.2010.08.016 . hal-00696566

HAL Id: hal-00696566

<https://hal.science/hal-00696566>

Submitted on 12 May 2012

HAL is a multi-disciplinary open access archive for the deposit and dissemination of scientific research documents, whether they are published or not. The documents may come from teaching and research institutions in France or abroad, or from public or private research centers.

L'archive ouverte pluridisciplinaire **HAL**, est destinée au dépôt et à la diffusion de documents scientifiques de niveau recherche, publiés ou non, émanant des établissements d'enseignement et de recherche français ou étrangers, des laboratoires publics ou privés.

Accepted Manuscript

Thermomechanical Properties of Copper-Carbon Nanofibre Composites Prepared by Spark Plasma Sintering and Hot Pressing

Jennifer M. Ullbrand, José M. Córdoba, Javier Tamayo-Ariztondo, María R. Elizalde, Mats Nygren, Jon M. Molina-Aldareguia, Magnus Odén

PII: S0266-3538(10)00324-6
DOI: [10.1016/j.compscitech.2010.08.016](https://doi.org/10.1016/j.compscitech.2010.08.016)
Reference: CSTE 4797

To appear in: *Composites Science and Technology*

Received Date: 17 November 2009
Revised Date: 22 June 2010
Accepted Date: 23 August 2010

Please cite this article as: Ullbrand, J.M., Córdoba, J.M., Tamayo-Ariztondo, J., Elizalde, M.R., Nygren, M., Molina-Aldareguia, J.M., Odén, M., Thermomechanical Properties of Copper-Carbon Nanofibre Composites Prepared by Spark Plasma Sintering and Hot Pressing, *Composites Science and Technology* (2010), doi: [10.1016/j.compscitech.2010.08.016](https://doi.org/10.1016/j.compscitech.2010.08.016)

This is a PDF file of an unedited manuscript that has been accepted for publication. As a service to our customers we are providing this early version of the manuscript. The manuscript will undergo copyediting, typesetting, and review of the resulting proof before it is published in its final form. Please note that during the production process errors may be discovered which could affect the content, and all legal disclaimers that apply to the journal pertain.



Thermomechanical Properties of Copper-Carbon Nanofibre Composites

Prepared by Spark Plasma Sintering and Hot Pressing

Jennifer M. Ullbrand¹, José M. Córdoba*¹, Javier Tamayo-Ariztondo², María R. Elizalde²
Mats Nygren³, Jon M. Molina-Aldareguia⁴ and Magnus Odén¹

¹Nanostructured Materials, Department of Physics, Chemistry, and Biology (IFM), Linköping University, 58183 Linköping, Sweden.

²CEIT and Tecnun (University of Navarra), Manuel de Lardizábal 15, 20018, San Sebastián, Spain

³Univ. Stockholm, Arrhenius Lab, Dept. Inorgan. Chem., S-10691 Stockholm, Sweden

⁴Fundación IMDEA-Materiales, c/Profesor Aranguren s/n, 28040 Madrid, Spain

ABSTRACT

Several types of carbon nanofibres (CNF) were coated with a uniform and dense copper layer by electroless copper deposition. The coated fibres were then sintered by two different methods, spark plasma sintering (SPS) and hot pressing (HP). The Cu coating thickness was varied so that different volume fraction of fibres was achieved in the produced composites. In some cases, the CNF were pre-coated with Cr for the improvement the Cu adhesion on CNF. The results show that the dispersion of the CNF into the Cu matrix is independent of the sintering method used. On the contrary, the dispersion is directly related to the efficiency of the Cu coating, which is tightly connected to the CNF type. Overall, strong variations of the thermal conductivity (TC) of the composites were observed (20-200 W/mK) as a function of CNF type, CNF volume fraction and Cr content, while the coefficient of thermal expansion (CTE) in all cases was found to be considerably lower than Cu (9.9-11.3 ppm/K). The results show a good potential for SPS to be used to process this type of materials, since the SPS samples show better properties than HP samples even though they have a higher porosity, in applications where moderate TC and low CTE are required.

Keywords: Carbon nanofibre, copper, metal matrix composite, thermal conductivity, coefficient of thermal expansion

Acknowledgements: Gerhard Traxler and Thomas Placzek from Dept. of Materials Technology, ARC Seibersdorf Research, and Dr. Volker Brüser and Sina Kutschera from Dept. Plasmaprozesstechnik, Leibniz-Institut für Plasmaforschung und Technologie e.V.

The Basque Government (project Etortek-inanogune, project PI-07/17) is also acknowledged for the funds received. J.T-A is grateful to the Basque Government for his PhD Grant.

The financial contribution of EU FP6 031712 INTERFACE project is gratefully acknowledged

*Corresponding Author. Phone: +46 13281780. E-mail address: josga@ifm.liu.se

ACCEPTED MANUSCRIPT

1. INTRODUCTION.

Composites (metal matrix composite (MMC), ceramic matrix composite (CMC)) are a class of engineering materials that offer opportunities to tailor properties and meet specific requirements[1-4], e.g. in heat spreaders. The ideal material for heat spreader applications combines a high thermal conductivity (TC) with a high heat capacity to absorb thermal spikes, and a low coefficient of thermal expansion (CTE), to remove heat from, for example, electronic circuit boards while avoiding stresses due to thermal cycling. Metals have a high thermal conductivity and hence are commonly used as heat spreaders, but their CTE is high [5, 6].

Materials such as CuMo, CuW, Al/SiC, AlN, FeNi, FeNiCo and diamond are usually used when a heat spreader with high TC and low CTE is needed. However, these materials suffer from various drawbacks, such as high density (MoCu, WCu), relatively high CTE (Al/SiC, AlN), poor thermal performance (FeNi, FeNiCo) and in the case of diamond, a high price [7, 8] and low machinability. Composite materials, especially metal matrix composites, have the potential to fulfill the requirements, because a careful control of the reinforcing filler to matrix ratio allows good adjustment of physical and mechanical properties [9]. In this context, carbon nanofibres (CNF) are currently being considered as a potential reinforcement for various composite materials due to their excellent mechanical, thermal, and electrical properties[10-14]. More specifically, CNF reinforced copper composites constitute an ideal candidate to work as an electrical contact material and/or substrate for semiconductor devices[15] due to their potentially high electrical and thermal conductivity, high wear resistance, low coefficient of thermal expansion, good machinability and low price.

One of the main difficulties to manufacture such a material resides on the poor wetting between copper and carbon, which makes it difficult to fabricate dense composites with homogeneously distributed fibres, through infiltration methods. It is anticipated that the

wetting problem could be overcome by coating the carbon nanofibre with copper before the consolidation process. Different coating techniques can be used, such as sputtering [16], electrodeposition [17, 18], wetness technique [19], but the method of choice for metallization and interconnection which has emerged in recent years is electroless deposition due to its low cost, fast deposition rate, good filling capability, good uniformity and low process temperatures [20-23]. The deposition of Cr interlayers onto the CNF before Cu deposition has also been explored with the objective of improving the adhesion of Cu on CNF. Cr is known to react with C and Cu to form the corresponding Cr-C carbide and Cr-Cu alloy. Previous work [24-26] have shown that the interface properties between C and Cu using Cr is improved by the presence of interlayers. The interlayer should although be thin since impurities in the Cu-matrix decrease the thermal conductivity.

Hence, in this paper we report on the fabrication of carbon nanofibre reinforced copper composites where the fibres are coated by electroless deposition prior to densification by spark plasma sintering or hot pressing. The difference between the used fibre types is how the relative orientation of the graphene sheets with respect to the fibre direction is aligned. The performance of the composites was evaluated in terms of their coefficient of thermal expansion and thermal conductivity.

2. EXPERIMENTAL.

Two types of carbon nanofibres have been used in the analysis: nanofibres with a herringbone structure (300 nm in diameter and specific surface area of 165 m²/g, Future Carbon GmbH) denoted HB and a platelet structure (150 nm in diameter and specific surface area of 72 m²/g, Future Carbon GmbH) denoted PL. In the PL CNF, the graphene sheets are perpendicular to the longitudinal direction, while they are inclined in the HB CNF. In some cases, the HB and PL fibres were heat treated at 3023 K for 30 min in helium atmosphere prior to the composite fabrication and those will be denoted HBHT and PLHT, respectively. With the intention of improving the Cu-C interface, some of the PLHT CNF were coated with Cr prior to the Cu electroless deposition. Cr was deposited by dc magnetron sputtering from a 99.95% pure Cr target resulting in a 24% weight increase of the fibres. These fibres are denoted PLCr.

The electroless copper deposition of the samples was carried out following the optimized parameters and reagents described by Cordoba et al. [22]. Sintering was performed using two different methods: spark plasma sintering SPS (Dr Sinter 2050) and hot pressing HP (Sintris 10STV). The SPS samples were manually pre-pressed and sintered in a 12 mm graphite die. The inside of the die and the punches were covered with a graphite layer. In the case of HP, the graphite punches in contact with the sample were covered by a layer of boron nitride to avoid reaction with the sample. The HP machine heats mainly by heating wires, but also apply a low intensity DC current through the die. Both SPS and HP temperatures were measured by pyrometer. Table I summarizes the different samples synthesized and the sintering conditions (maximum temperature, holding time and pressure).

The morphology of the surfaces of the samples, polished down to 1 μm diamond paste, were determined by optical microscopy (Olympus BX 60 equipped with a digital camera (Olympus E410)) and scanning electron microscopy (JEOL LEO 1550 Gemini).

X-ray diffractograms (Philips PW-1729) of powders and polished surfaces were recorded with Cu K_{α} radiation over $41-47^{\circ} 2\Theta$ range and the FWHM of the Cu (111) diffraction peak was used for calculating the average diameter of the coherent diffracting domain according to the Scherrer equation [27].

The density of the CNF was determined by pycnometry [28] in an AccuPyc 1330. The equipment was calibrated with a standard volume. Each run consisted of ten He- purges prior to five readings of the sample volume. The average volume was used to extract the density of the five measurements. The standard deviation of one run was less than 0.0008 cm^3 for sample volumes in the range of $0.1119-0.8223 \text{ cm}^3$.

The bulk densities of the sintered composites were measured by the water immersion technique (Archimedes' method) using a Sartorius ME2359 balance and taking the temperature effect on the water density into account. The maximum achievable densities were estimated based on the rule of mixtures.

The thermal diffusivity of the composites was measured at room temperature in air using an ordinary light flash and an infrared (IR) camera. A light sensor coupled to an oscilloscope tracked the starting point of the measurement. The thermal diffusivity values were determined based on the time to reach half of the maximum temperature on the rear side of the sample and the sample thickness[29]. The thermal conductivity was calculated according to the following equation[30, 31]:

$$TC = \kappa (\rho_{\text{Cu}} C_{\text{Cu}} f_{\text{Cu}} + \rho_{\text{CNF}} C_{\text{CNF}} f_{\text{CNF}} + \rho_{\text{Cr}} C_{\text{Cr}} f_{\text{Cr}}) \quad (1)$$

where TC is the thermal conductivity, κ is the measured thermal diffusivity, ρ_{CNF} and ρ_{Cu} are the densities of the copper and carbon nanofibre, respectively, and f_{Cu} and f_{CNF} are the

volume fractions of copper and carbon nanofibre, respectively. The specific heat capacities, C_{CNF} , C_{Cu} , and C_{Cr} used for the fibres, copper and chromium were 930, 385, and 450 J/kgK respectively.

The coefficients of thermal expansion were determined with a dilatometer (Netzsch DIL 402C). Heating cycles were performed in He atmosphere from room temperature to 300°C with a heating and cooling rate of 10 °C/min. The coefficient of thermal expansion, CTE, was extracted from the linear slope according to equation 2[32-34]:

$$\Delta L/L = \text{CTE } \Delta T \quad (2)$$

where, L is the initial specimen length, ΔL is its dilatation and ΔT is the temperature increase.

3. RESULTS AND DISCUSSION

The densities of the as-received and treated CNF fibres determined by pycnometry were: 2.21 g/cm³ for the CNF-HB, 2.24 g/cm³ for the CNF-PL, 2.18 g/cm³ for the CNF-HBHT, and 2.17 g/cm³ for the CNF-PLHT. The density of the PLCr powder was calculated by the rule of mixtures, using the experimental density value for the CNF-PL and the standard density of Cr (7.14 g/cm³) resulting in a value of 2.68 g/cm³.

The morphology of the as received and heat treated CNF with and without Cu coatings have been reported elsewhere[14, 22]. In general, Cu depositions onto heat treated CNF (HBHT, PLHT, and PLCr) results in a complete coverage of the fibres while as received fibres show some naked areas. This is an effect of the reorientation of the outermost graphite sheets during heat treatment and the addition of Cr, which promotes the adhesion of Cu to the CNF.

The measured densities of the metal matrix composites are presented in Table II. As expected, the density decreases linearly with CNF reinforcement since the total density is the volume fraction average of the density of the matrix and reinforcements. The measured densities for the 7%_{wt}, 14%_{wt} and 24%_{wt} reinforcement of CNF were 6-7 g/cm³, 4.5-6.0 g/cm³ and 4.0-5.5 g/cm³, respectively. The composite density is strongly affected by the choice of sintering method, with HP displaying significantly higher densities (95-100 %) than SPS (82-97 %).

The size of the Cu crystallites, determined by the Scherrer equation, is shown in Table II. Samples sintered by SPS show smaller crystallite sizes than those sintered by HP. This is a consequence of the higher temperatures used during the hot pressing process. The dispersion of the CNF in the Cu matrix was assessed by optical microscopy. Micrographs in Figure 1(a) to (e) show examples over sample surfaces, where darker areas represent higher CNF content

and brighter areas represent higher content of copper. In all cases, the CNF dispersion observed was homogeneous, with the exception of some agglomerates seen for both of the sintering methods used. The main difference in dispersion is connected to the type of CNF used. For instance, the CNF agglomerates observed were few but large (350 μm) for PL CNF, while for HB CNF the agglomerates were observed more frequently but with a smaller size (60 μm) see Figure 1 (a) and (b). The samples with heat treated CNF and PLCr show the least agglomeration (Figure 1 (c) and (e) compared to untreated fibres Figure 1 (a) and (d)). The amount of fibre agglomeration in the composites is directly related to the Cu-coating process, so that the best fibre dispersion is achieved for the most homogeneously Cu coated fibres.

Figure 1 (f) and (g) show SEM images of the composite processed by HP using 24% HB CNF (sample HP-HB24) and by SPS using 14% PLHT CNF (sample HP-PLHT14) respectively. In Figure 1(f) a clear preferential orientation of the CNF in planes perpendicular to the pressing direction is observed, which has previously been documented as a consequence of the uniaxial pressing, [35-37]. Figure 1(g) shows the interface between the Cu matrix and a fibre. Despite the poor wetting between C and Cu[38], a dense C/Cu interface was achieved. No interdiffusion or segregation over large distances ($> 1 \mu\text{m}$) could be detected by energy dispersive x-ray spectroscopy (EDX). However, reactions at the interface cannot be excluded, especially in the presence of Cr.

Table II summarises the values of the thermal diffusivity measured parallel to the prior pressing direction. A large variation between 3 and 60 mm^2/s is observed depending on the CNF type, volume fraction and sintering method. Figure 2 shows the thermal conductivity of the samples and similar dependences are seen here. Due to the presence of chromium, the weight fraction of CNF for the PLCr samples is 6%, 10% and 18%, instead of 7%, 14% and 24%, which is the case for the other samples. The thermal conductivity decreases sharply with increasing weight fraction of fibres. Hence the maximum thermal conductivity is observed for

PLCr6 with ~ 200 W/Km, which is considerably lower than pure Cu (385 W/Km) but substantially higher than what has been observed for Cu/CNF composites before [39].

The decrease in thermal conductivity with respect to pure Cu might come from several factors: (i) the crystal quality of the CNF, (ii) the orientation of the graphene planes within the CNF, (iii) the interfacial thermal resistance of the Cu-C interface, (iv) alignment of the CNF in the pressing direction during processing, (v) inhomogeneous fibre dispersion and (vi) the amount of porosity in the final composite.

First of all, considering the expected anisotropy of the CNF and the observed preferred alignment of the CNF, perpendicular to the pressing direction, we expect a higher conductivity in the perpendicular pressing direction than in the parallel pressing direction of the sample. However, the thermal conductivity was only measured in the parallel direction due to constraints in the sample size. Therefore, the measured thermal conductivities should be interpreted with caution. For instance, the strong decrease in thermal conductivity with CNF volume fraction could be attributed to this anisotropy effect, especially when considering that no major changes have been observed in density and/or CNF dispersion with volume fraction.

Even with the limitations addressed above, the relative differences in thermal conductivity observed raise some interesting points. For instance, the HB fibres are more bent and entangled than PL fibres [22] resulting in a decrease in the net heat transport which could explain why the thermal diffusivity values of the PL composites are better. The dramatic effect of the high temperature heat treatment of the CNF is due to the graphitisation [14], which results in improved Cu deposition efficiency. Finally, it is also clear from the results that the introduction of a Cr interlayer between the Cu and the CNF has a beneficial effect on the thermal conductivity of the composite, at least in the samples processed by SPS. This is likely due to the improvement of Cu adhesion onto the Cr-C interface, resulting in an improved Cu coating process and a reduction of the thermal resistance of the interface.

However, in the samples processed by HP, the beneficial effect of the Cr addition is not that clear. In this case, the processing temperatures are considerably higher and it is well known that the dissolution of Cr into the Cu matrix would have a detrimental effect on the thermal properties.

Table III summarizes the coefficients of thermal expansion (CTE) of selected samples, measured from room temperature to 250°C. The CTE of the Cu/CNF composite depends upon the CNF type, the volume fraction of CNF, the CNF orientation, the quality of the dispersion, the porosity, and the interface resistance. In all studied cases, the CTE values are in a narrow range, 9.9-11.3 ppm/K, independently of the fibre content and the sintering method. The addition of Cr on the CNF surface results in a decrease in the CTE (PLCr6: HP, 10.1 ppm/K; PLCr6: SPS, 9.9 ppm/K), which is consistent with the expected improved Cu adhesion. Overall and compared with other techniques (powder metallurgy[40, 41], tape casting[42], copper salt chemical decomposition[39]), electroless copper deposition as a pre step before sintering has been shown to be a superior method for the enhancement of the thermomechanical properties of CNF/Cu composites. Also when comparing with other Cu reinforcement materials[42, 43] such as with SiC[44], W[45], AlN[46] and with Mo[47], the carbon nanofibres have shown better thermal conductivity and lower CTE.

We note that, although SPS samples in general show lower relative density (higher residual porosity) than the HP samples they display comparable values of thermal conductivity and CTE. The spark plasma sintering and hot pressing parameters (temperature, pressure and holding time) affect the interface between CNF and copper as well as the CNF degradation, therefore further detailed studies of the C-Cu interface is needed in order to understand the influence of the chosen sintering method. An explanation for the higher densities but worse properties for the HP samples might be the high compressing temperatures and pressures that can cause Cr and Cu to melt and flow away from the CNF

surface reducing the interface properties and thermal conductivity. The effect of the current in the SPS sintering is relatively unknown and might influence the interfacial properties as well. However, our results suggest that the SPS technique is a promising sintering method to obtain superior composites for heat spreader applications, since further densification would yield an even higher thermal conductivity. Additionally, the use of highly graphitic fibres (fibres subjected to high temperature pre-treatment) is preferable.

ACCEPTED MANUSCRIPT

4. CONCLUSIONS

In this paper we report on the fabrication of carbon nanofibre reinforced copper composites where the fibres are coated by electroless deposition prior to densification by spark plasma sintering or hot pressing, using different types of CNF: platelet PL, herringbone HB, before and after a high temperature (HBHT and PLHT) graphitization process, and also CNF precoated with Cr (PLCr).

Compared with conventional powder metallurgy and infiltration techniques, a very good dispersion of the CNF into the Cu matrix can be achieved with this approach, independently of the sintering method used. The results show that the quality of the dispersion depends on the efficiency and homogeneity of the Cu coating, which depends on the CNF type, HB shows the worst dispersion while HBHT, PLHT and PLCr shows superior dispersion.

SPS sintering, which is carried out at considerably lower temperatures (550-650°C) than hot pressing (750-975°C), results in slightly lower densities, but the final thermal properties obtained for both routes are comparable. This indicates that the SPS technique stabilizes the adhesion of Cu on the Cr-C interface possibly by the current or by the lower operating temperature. The SPS sintering technique is therefore, according to this study, the more promising sintering method. Overall, strong variations of the thermal conductivity of the composites were observed (20-200 W/mK) as a function of CNF type, CNF volume fraction and Cr content, while the coefficient of thermal expansion (CTE) in all cases was found to be considerably lower than Cu (9.9-11.3 ppm/K).

The highest thermal conductivity (194 W/Km) was obtained for Cr pre-coated CNF and a weight fraction of 6% processed by SPS. All in all, the results show a good potential for SPS to be used to process this type of materials in applications where moderate thermal conductivity and low CTE are required.

5.- REFERENCES

- [1] Chu K, Liu ZF, Jia CC, Chen H, Liang XB, Gao WJ, Tian WH, Guo H. Thermal conductivity of SPS consolidated Cu/diamond composites with Cr-coated diamond particles. *J. Alloys Comp.* 2010; 490:453.
- [2] Chu K, Wu QY, Jia CC, Liang XB, Nie JH, Tian WH, Gai GS, Guo H. Fabrication and effective thermal conductivity of multi-walled carbon nanotubes reinforced Cu matrix composites for heat spreader applications. *Comp. Sci. Tech.* 2010; 70:298.
- [3] Cordoba JM, Sanchez-Lopez JC, Aviles MA, Alcala MD, Gotor FJ. Properties of Ti(C,N) cermets synthesized by mechanically induced self-sustaining reaction. *J Eur Ceram Soc* 2009;29:1173.
- [4] Waku Y, Nakagawa N, Wakamoto T, Ohtsubo H, Shimizu K, Kohtoku Y. A ductile ceramic eutectic composite with high strength at 1,873 K. *Nature* 1997; 389: 49.
- [5] Asthana R. Processing effects on the engineering properties of cast metal-matrix composites. *Adv. Perform. Mater.* 1998; 5: 213.
- [6] Legzdins CF, Samarasekera IV, Meech JA. MMCX - An expert system for metal matrix composite selection and design. *Canadian Metall. Quart.* 1997; 36: 177.
- [7] Hammel E, Tang X, Trampert M, Schmitt T, Mauthner K, Eder A, Potschke P. Carbon nanofibers for composite applications. *Carbon.* 2004; 42: 1153.
- [8] Kitzmantel M. Wetting and infiltration behaviour of copper and copper alloys on carbon nanofibers. Master thesis 2008;Vienna University of Technology.
- [9] Chung DDL. Materials for thermal conduction. *Appl. Therm. Eng.* 2001; 21: 1593.
- [10] Endo M, Kim YA, Hayashi T, Nishimura K, Matusita T, Miyashita K, Dresselhaus MS. Vapor-grown carbon fibers (VGCFs) - Basic properties and their battery applications. *Carbon.* 2001; 39: 1287.
- [11] Carneiro OS, Covas JA, Bernardo CA, Caldeira G, Van Hattum FWJ, Ting JM, Alig RL, Lake ML. Production and assessment of polycarbonate composites reinforced with vapour-grown carbon fibres. *Comp. Sci. Tech.* 1998; 58: 401.
- [12] Heremans J, Beetz CP. Thermal conductivity and thermopower of vapor grown graphite fibres. *Phys. Review B.* 1985; 32: 1981.
- [13] Heremans J. Electrical conductivity of vapor-grown carbon-fibres. *Carbon* 1985; 23: 431.
- [14] Cordoba JM, Tamayo-Ariztondo J, Molina-Aldareguia JM, Elizalde MR, Oden M. Morphology influence of the oxidation kinetics of carbon nanofibers. *Corros. Sci.* 2009; 51: 926.
- [15] Ngo Q, Cruden BA, Cassell AM, Sims G, Meyyappan M, Li J, Yang CY. Thermal interface properties of Cu-filled vertically aligned carbon nanofiber arrays. *Nano Letters* 2004; 4: 2403.
- [16] Neubauer E, Korb G, Eisenmenger-Sittner C, Bangert H, Chotikaprakhan S, Dietzel D, Mansanares AM, Bein BK. The influence of mechanical adhesion of copper coatings on carbon surfaces on the interfacial thermal contact resistance. *Thin Solid Films.* 2003; 433: 160.
- [17] Arai S, Endo M. Carbon nanofiber-copper composite powder prepared by electrodeposition. *Electrochem. Commun.* 2003; 5: 797.
- [18] Wan YZ, Wang YL, Luo HL, Dong XH, Cheng GX. Effects of fiber volume fraction, hot pressing parameters and alloying elements on tensile strength of carbon fiber reinforced copper matrix composite prepared by continuous three-step electrodeposition. *Mater. Sci. Eng. A.* 2000; 288: 26.

- [19] Ma J, Park C, Rodriguez NM, Baker RTK. Characteristics of copper particles supported on various types of graphite nanofibers. *J. Phys. Chem. B.* 2001; 105: 11994.
- [20] Yung EK, Romankiw LT, Alkire RC. Plating of copper into through-holes and vias. *J. Electrochem. Soc.* 1989; 136: 206.
- [21] Lu W, Donepudi VS, Prakash J, Liu J, Amine K. Electrochemical and thermal behavior of copper coated type MAG-20 natural graphite. *Electrochim. Acta* 2002; 47: 1601.
- [22] Cordoba JM, Oden M. Growth and characterization of electroless deposited Cu films on carbon nanofibers *Surf. Coat. Tech.* 2009; 203: 3459.
- [23] Mallory O, Hajdu JB. *Electroless plating. Fundamentals and Applications.* ed. Noyes Publications/William Andrew Publishing, LLC, New York 1990; Chapter 12. pp. 289–389.
- [24] Mayerhofer KE, Neubauer E, Eisenmenger-Sittner C, Hutter H. Adhesion promotion of Cu on C by Cr intermediate layers investigated by the SIMS method. *Anal. Biochem. Chem.* 2002; 374: 602.
- [25] Mortimer DA, Nicholas M. The wetting of carbon and carbides by copper alloys. *J. Mater. Sci.* 1973; 8: 640.
- [26] Mortimer DA, Nicholas M. The wetting of carbon by copper and copper alloys. *J. Mater. Sci.* 1970; 5: 149.
- [27] Scherrer P. Estimation of the size and internal structure of colloidal particles by means of röntgen. *Nachr. Ges. Wiss. Göttingen* 1918; 2: 96.
- [28] Viana M, Jouannin P, Pontier C, Chulia D. About pycnometric density measurements. *Talanta.* 2002; 57: 583.
- [29] Nagpure SC, Dinwiddie R, Babu SS, Rizzoni G, Bhushan B, Frech T. Thermal diffusivity study of aged Li-ion batteries using flash method. *J. Power Sour.* 2010; 195: 872.
- [30] Araki N, Tang DW, Makino A, Hashimoto M, Sano T. Transient characteristics of thermal conduction in dispersed composites. *Int. J. Thermo.* 1998; 19: 1239.
- [31] Kerrisk JF. *Thermal Diffusivity of Heterogeneous Materials. 2 Limit of Steady-State Approximation.* *J. Appl. Phys.* 1972; 43: 112.
- [32] Hummel RE. *Electronics Properties of Materials.* 1994; Springer-Verlag: 134.
- [33] Barsoum MW. *Fundamentals of Ceramics.* Series in Materials Science and Engineering 2003; ed. Taylor and Francis: pp. 94.
- [34] Nix FC, MacNair D. The thermal expansion of pure metal: Copper, Gold, Aluminium Nickel, and Iron. *Phys. Review.* 1941; 60: 597.
- [35] Barcena J, MaudeSa J, Coletoa J, Baldonado JL, de Salazar JMG. Microstructural study of vapour grown carbon nanofibre/copper composites. *Comp. Sci. Tech.* 2008; 68: 1384.
- [36] Korb G, Buchgraber W, Schubert t. Properties and microstructure of short carbon fibre reinforced copper matrix composites. In: 21st International Spring Seminar on Electronics Technology Conference Proceedings 1998; Neusiedl, Australia: p. 116.
- [37] Geffroy PM, Silvain JF. Structural and thermal properties of hot pressed Cu/C matrix composites materials used for the thermal management of high power electronic devices. *Mater. Sci. Forum* 2007; 534-536: 1505.
- [38] Lee SB, Matsunaga K, Ikuhara Y, Lee SK. Effect of alloying elements on the interfacial bonding strength and electric conductivity of carbon nano-fiber reinforced Cu matrix composites. *Mater. Sci. Eng. A.* 2007; 449: 778.
- [39] Silvain JF, Vincent C, Heintz JM, Chandra M. Novel processing and characterization of Cu/CNF nanocomposite for high thermal conductivity applications. *Comp. Sci. Tech.* 2009; 69; 2474.
- [40] Korab J, Stefanik P, Kavecky S, Sebo P, Korb G. Thermal conductivity of unidirectional copper matrix carbon fibre composites. *Compos. Part A.* 2002; 33: 577.

- [41] Prakasan K, Palaniappan S, Seshan S. Thermal expansion characteristics of cast Cu based metal matrix composites. *Compos. Part A*. 1997; 28: 1019.
- [42] Geffroy PM, Chartier T, Silvain JF. Preparation by tape casting and hot pressing of copper carbon composites films. *J. Eur. Ceram. Soc.* 2007; 27: 291.
- [43] Kang JL, Nash P, Li JJ, Shi CS, Zhao NQ. Achieving highly dispersed nanofibres at high loading in carbon nanofibre-metal composites. *Nanotech.* 2009; 20: 235607.
- [44] Schubert T, Trindade B, Weissgarber T, Kieback B. Interfacial design of Cu-based composites prepared by powder metallurgy for heat spreader applications. *Mater. Sci. Eng. A*. 2008; 475: 39.
- [45] German RM. A model for the thermal properties of liquid phase sintered composites. *Metall. Trans. A*. 1993; 24: 1745.
- [46] Lee KM, Oh DK, Choi WS, Weissgarber T, Kieback B. Thermomechanical properties of AlN-Cu composite materials prepared by solid state processing. *J. All. Comp.* 2007; 434: 375.
- [47] Wu H, Wang Z, Zheng Q, Zhou J. *China Molybdenum Industry* 2006;30:30.

Figure Caption

Figure 1. Representative optical images of the samples, (a) HP-PL7, (b) HP-HB7. (c) SPS-PLHT7, (d) SPS-PL14, (e) SPS-PLCr14, (f) Characteristic SEM image of HP-HB sample 24, (g) high-res SEM image of the sample SPS-PLHT14 showing one fibre with EDX inset.

Figure 2. Thermal conductivity of the composites reinforced with Platelet (PL) and Herringbone (HB) CNF as received, heat treated and coated with Cr by PVD (only for PL) for three weight fractions: 7, 14 and 24%.

ACCEPTED MANUSCRIPT

Table I. Summary of the sample compositions (HB, CNF-herringbone; PL, CNF-platelet; HBHT, CNF-herringbone heat treated; PLHT, CNF-platelet heat treated and PLCr, CNF-platelet previously coated with Cr by PVD) and used experimental conditions (T, temperature; p, pressure; t_{hold} , holding time)

Sample ID	Composition (% wt.)	SPS			HP		
		T (°C)	P (MPa)	t_{hold} (min)	T (°C)	P (MPa)	t_{hold} (min)
HB7	7%CNF _{HB} +93%Cu	600	50	5	850	122	3
HB14	14%CNF _{HB} +86%Cu	600	50	5	900	100	3
HB24	24%CNF _{HB} +76%Cu	600	100	5	975	122	4.2
PL7	7%CNF _{PL} +93%Cu	600	50	5	750	80	3
PL14	14%CNF _{PL} +86%Cu	600	50	5	800	100	3
PL24	24%CNF _{PL} +76%Cu	650	100	3	975	138	3
HBHT7	7%CNF _{HBHT} +93%Cu	600	50	5	750	122	3
HBHT14	14%CNF _{HBHT} +86%Cu	600	50	5	900	100	3
HBHT24	24%CNF _{HBHT} +76%Cu	650	100	3	975	122	4.2
PLHT7	7%CNF _{PLHT} +93%Cu	600	50	5	750	80	3
PLHT14	14%CNF _{PLHT} +86%Cu	600	50	5	900	100	3
PLHT24	24%CNF _{PLHT} +76%Cu	650	100	3	-	-	3
PLCr6	6%CNF _{PL} +92.7%Cu+1.3%Cr	600	50	5	750	100	3
PLCr10	10%CNF _{PL} +87.8%Cu+2.2%Cr	600	50	5	900	122	3
PLCr18	18%CNF _{PL} +78%Cu+4%Cr	550	100	1	975	138	3

SPS, Spark Plasma Sintering; HP, Hot Pressing

Table II. Real density [$\pm 0.2\%$] and relative density, crystallite size and thermal diffusivity [$\pm 1\%$] of the samples studied.

Sample ID	SPS			HP		
	Density [g/cm^3] (%relative)	Cu [D] [nm]	κ [$10^{-6} \text{ m}^2/\text{s}$]	Density [g/cm^3] (%relative)	Cu [D] [nm]	κ [$10^{-6} \text{ m}^2/\text{s}$]
HB7	5.96 (89%)	117	14.2	6.46 (96%)	199	22.8
HB14	4.54 (82%)	108	4.2	5.41 (97%)	217	13.9
HB24	3.82 (85%)	80	3.8	4.30 (100%)	135	10.4
PL7	6.22 (94%)	111	36.2	6.49 (98)	333	43.6
PL14	5.40 (93%)	45	14.8	5.72 (98%)	183	20.4
PL24	4.37 (95%)	104	6.9	4.88 (100%)	221	13.9
HBHT7	6.49 (91%)	115	47.2	6.77 (95%)	341	49.4
HBHT14	5.50 (90%)	118	20.5	6.12 (100%)	236	28.8
HBHT24	4.61 (97%)	74	9.6	5.31 (100%)	166	4.6
PLHT7	6.21 (92%)	115	45.1	6.58 (97%)	238	43.5
PLHT14	5.23 (88%)	106	25.8	5.85 (99%)	153	29.0
PLHT24	3.85 (84%)	92	3.8	-	-	-
PLCr6	6.70 (95%)	98	59.5	6.97 (99%)	192	30.7
PLCr10	5.29 (94%)	110	26.2	5.92 (100%)	198	23.8
PLCr18	4.72 (84%)	105	17.8	5.45 (97%)	137	21.3

Table III. Thermal conductivity (TC) [$\pm 1\%$] and normal coefficient of thermal expansion (CTE) [$\pm 1\%$] from room temperature (rt) to 250°C measured parallel to the pressing direction.

Only the composites showing the highest thermal conductivity are reported.

Sample	TC [W/Km]	CTE [10^{-6} K^{-1}]	Relative density [%]	Processing conditions	
		rt→250°C		T (°C)	P (MPa)
PL7 (HP)	144.7	13.1	98	750	80
PL7 (SPS)	115.2	10.3	94	600	50
HBHT7 (HP)	171.8	10.4	96	750	122
HBHT7 (SPS)	157.3	11.5	89	600	50
PLHT7 (HP)	147.1	12.7	97	750	80
PLHT7 (SPS)	144.0	10.2	92	600	50
HBHT14 (HP)	106.2	11.0	100	900	100
PLHT14 (HP)	102.5	11.9	99	900	100
PLCr6 (HP)	104.5	10.1	99	750	100
PLCr6 (SPS)	194.6	9.9	95	600	50

Sample sintered by hot pressing (HP) or spark plasma sintering (SPS)

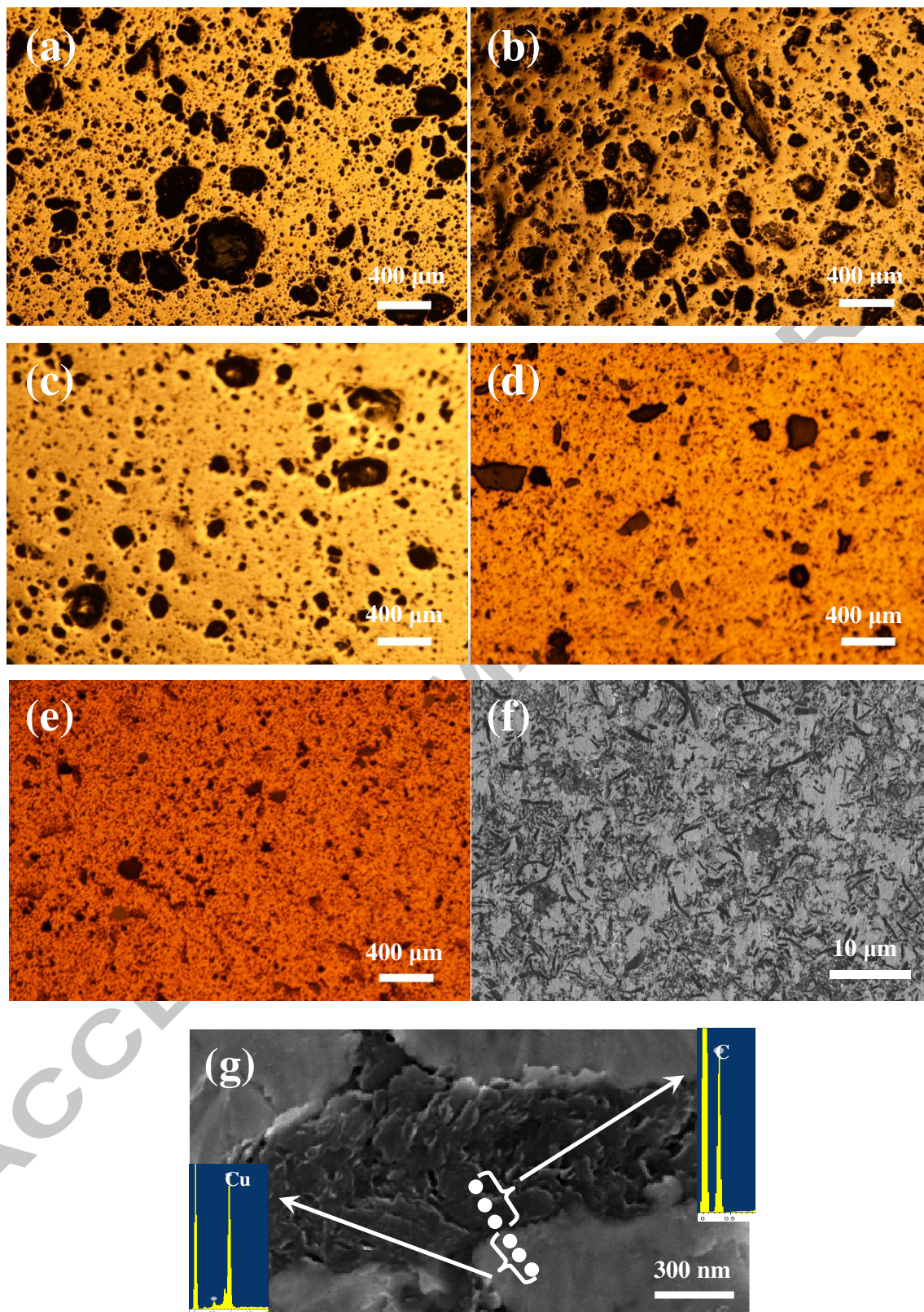


Figure 1

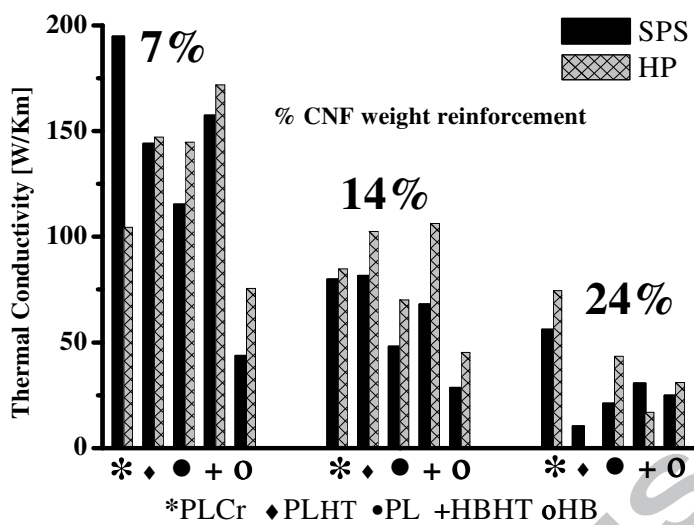


Figure 2